

Electronic Supporting Information

**Supramolecular interface decoration on polymer conductor for intrinsically stretchable near-infrared photodiode**

Fan Chen,<sup>a</sup> Yiming Li,<sup>a</sup> Yan Chen,<sup>a</sup> Yi-Xuan Wang<sup>\*a,b</sup> and Wenping Hu<sup>\*a,b</sup>

<sup>a</sup>Tianjin Key Laboratory of Molecular Optoelectronic Sciences, Department of Chemistry, School of Science, Tianjin University and Collaborative Innovation Center of Chemical Science and Engineering, Tianjin 300072, P. R. China.

<sup>b</sup>Haihe Laboratory of Sustainable Chemical Transformations, Tianjin 300192, P. R. China.

\*Email: huwp@tju.edu.cn; yx\_wang@tju.edu.cn

Contents

1. Experimental Section
2. Mechanical properties of SPC films
3. Electrical properties of SPC films
4. Transparency of SPC films
5. Mechanical properties of DPS films
6. Characterizations of OPD devices on rigid substrates
7. Characterizations of stretchable OPD devices
8. References

## 1. Experimental Section

**Materials.** PEDOT:PSS (Clevios PH 1000), PEDOT:PSS (Clevios AI 4083), polyethylene glycol tert-octylphenyl ether (Triton X-100), poly(ethylene glycol) diacrylate (PEGDA,  $M_n$  10,000) and [6,6]-phenyl-C<sub>70</sub>-butyric acid methyl ester (PC<sub>70</sub>BM) were obtained from Sigma-Aldrich. PEIE, Capstone™ FS-30 and poly[2,5-(2-octyldodecyl)-3,6-diketopyrrolopyrrole-*alt*-5,5-(2,5-di(thien-2-yl)thieno[3,2-b]thiophene)] (DPP-DTT) was purchased from Meryer, Chemours and 1-Material, respectively. Polyrotaxane plasticizer (PR) was synthesized referring to reported literatures.<sup>1-3</sup> All reagents and solvents in this experiment were purchased and used without further purification.

**Preparation of PR/PEDOT:PSS (PPR) films.** For the SEBS substrate preparation, a SEBS solution in toluene (200 mg/mL) was drop casted onto a silicon wafer, which was dried overnight at room temperature. A PPR solution contains 1 mL of PEDOT:PSS (PH1000), 50 mg of PR, 1 mg of photoinitiator (lithium phenyl(2,4,6-trimethylbenzoyl)phosphinate), and 1 wt% of Capstone™ FS-30. The PPR solution was spin coated on the UVO-treated SEBS substrate, and the resulting film was exposed under 365 nm UV light for 30 min. The conducting films before and after post-treatment with methanol were named of PPR and PPR-M, respectively.

**Preparation of SPC and composite anode films.** A solution of PEIE (0.2 wt%) in methanol was spin coated onto the PPR-M film (SPC) in air at 5000 rpm for 30 s, followed by annealing at 100 °C for 10 min. A solution of PEDOT:PSS (AI 4083) containing 5 vol% of Triton X-100 was spin coated onto the PPR film (composite anode) in air at 5000 rpm for 30s, followed by annealing at 100 °C for 10 min.

**Fabrication of OPD on a rigid substrate.** The glass substrate was ultrasonically cleaned in deionized water, acetone, and isopropanol sequentially for 10 minutes. Then, the cleaned glass substrate was treated with oxygen plasma for 10 minutes. A PPR solution was spin-coated on the glass substrate at 3000 rpm for 60 s, and the resulting film was exposed under UV light for 30 min. A solution of PEIE (0.2 wt%) in methanol

was then spin-coated at 5000 rpm for 30 s, followed by annealing at 100 °C for 10 min. The DPP-DTT:PC<sub>70</sub>BM:SEBS blends with different SEBS contents (0%, 29%, 44%, 55%) were dissolved in 1,2-dichlorobenzene and then was spin-coated at 1500 rpm for 60 s, followed by annealing at 100 °C for 60 min. The composite anode was prepared on a SEBS substrate, which was flipped over and laminated onto the DPS-44 film to yield the OPD device.

**Fabrication of intrinsically stretchable NIR-OPD.** The SPC and composite anode were prepared on SEBS substrates, respectively. The DPS-44 film was transferred onto the top of SPC by using a PDMS stamp. Finally, the SEBS/composite anode was flipped over and laminated onto the DPS-44 film. The stretchable OPD was peeled off from the glass holder before further test.

**Characterization.** The tensile properties of all films were tested by transferring the film to a SEBS substrate and then observed under optical microscope. Optical images were captured by Nikon Eclipse Ci-POL polarized microscope. Out-of-plane results of DPSs were obtained by Rigaku SmartLab X-ray diffractometer. The UV-vis absorption spectra and transmittance of PR/PEDOT:PSS films were measured with a SHZMADZU UV-3600 Plus spectrophotometer. The absorption spectra were normalized by film thickness. X-ray photoelectron spectroscopy (XPS) and Raman Spectroscopy were carried out by Thermo Fisher Scientific ESCALAB 250Xi and Thermo Fisher micro Raman imaging spectrometer Dxr2i, respectively. AFM images, work function and elastic moduli were measured on a Bruker Dimension Icon instrument. The current density–voltage ( $J$ – $V$ ) characteristics of the OPDs were evaluated using a Keithley 2636 source meter. The device area of the stretching was calculated using the Poisson's ratio of SEBS of 0.5. A light-emitting diode operating at 808 nm was used as the illumination source.  $R$ ,  $D^*$ , and linear dynamic range (LDR) of devices were calculated with reference to the reported literature.<sup>4</sup>

## 2. Mechanical properties of SPC films

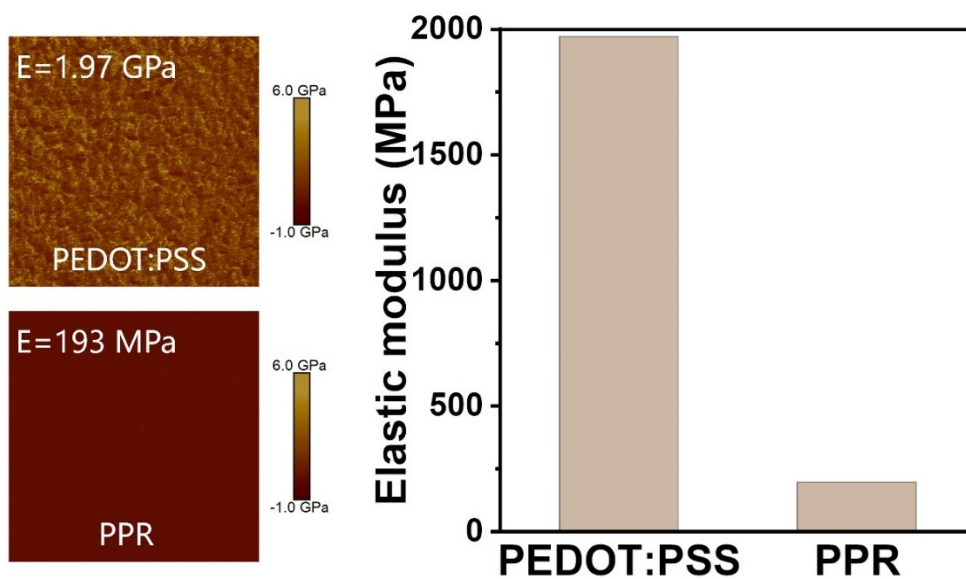


**Fig. S1** Derjaguin-Muller-Toporov (DMT) modulus images of PEDOT:PSS and PPR films obtained by the PFQNM.

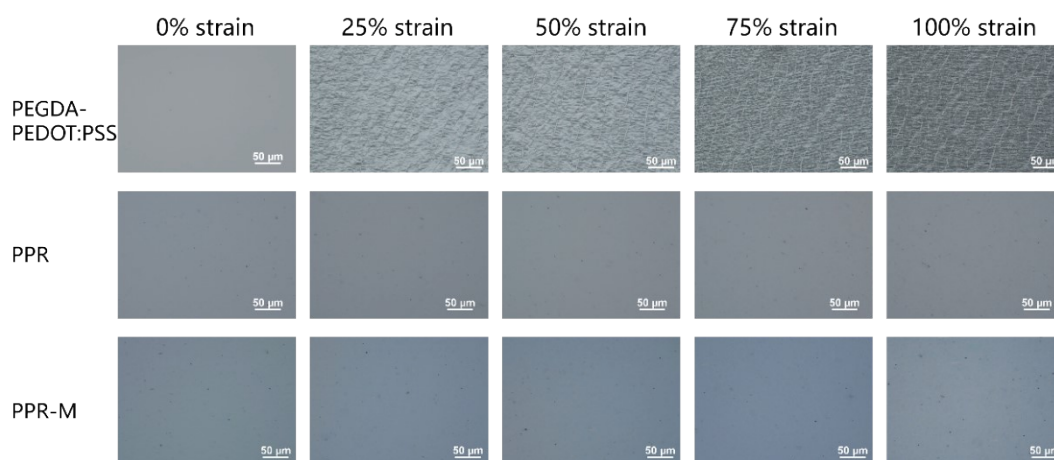


**Fig. S2** Optical microscope images of different PEDOT:PSS blend films on SEBS substrates at different strains.

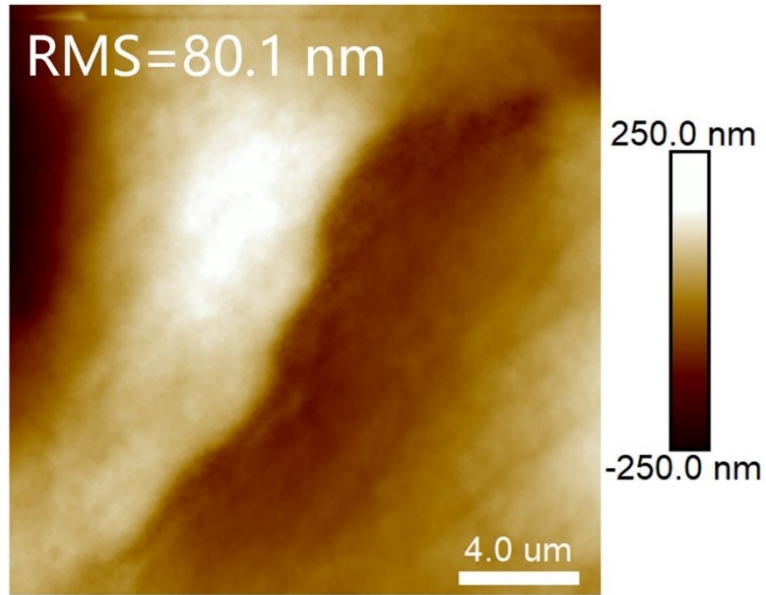


Fig. S3 AFM height image of PEGDA-PEDOT:PSS film by tapping mode.

### 3. Electrical properties of SPC films

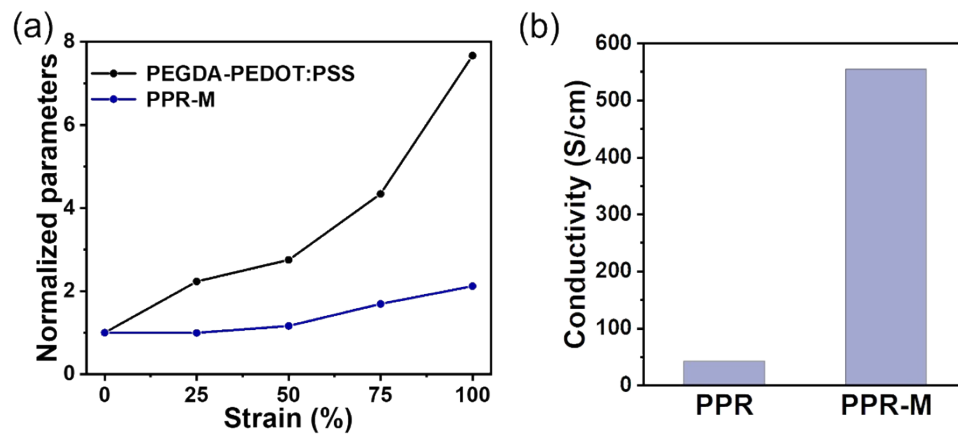
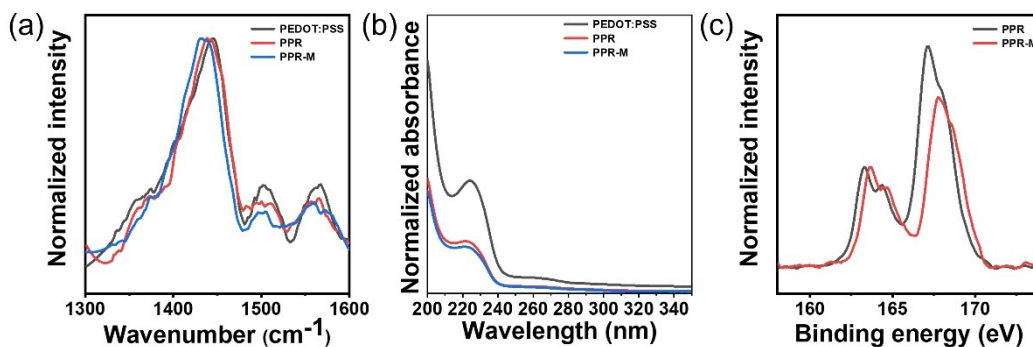
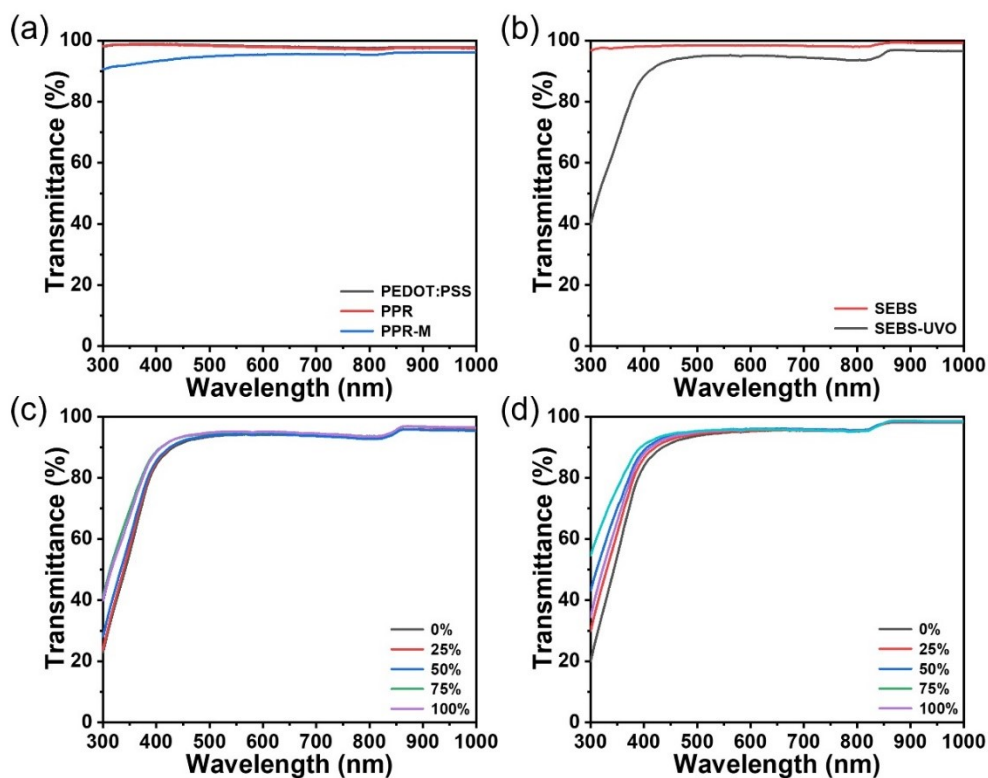


Fig. S4 (a) Relative resistance of PEGDA-PEDOT:PSS and PPR-M films depending on strains. (b) Conductivities of PR-PEDOT:PSS and PPR-M films.



**Fig. S5** (a) Raman spectra, (b) UV-vis spectra, and (c) XPS spectra for PPR films with and without methanol treatment.

#### 4. Transparency of SPC films



**Fig. S6** Optical transmittance of (a) PEDOT:PSS, PPR and PPR-M films, and (b) SEBS substrates with and without UVO treatment. Optical transmittance of (c) PPR-M on UVO-treated SEBS substrates, and (d) UVO-treated SEBS substrates at different strains.

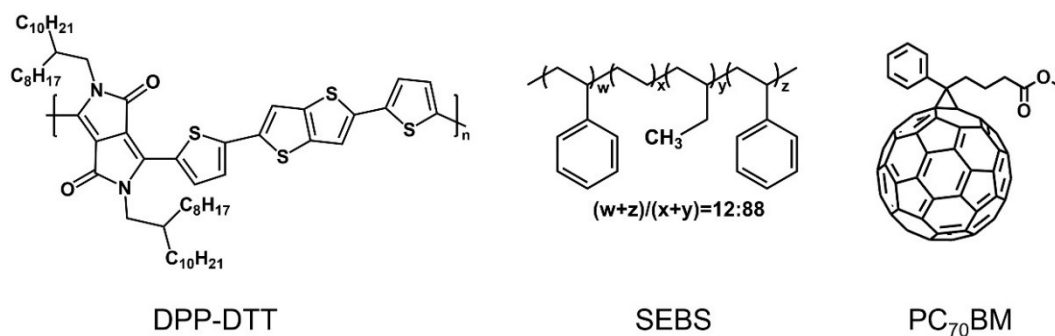


**Fig. S7** Chemical structures of materials used in DPS films.

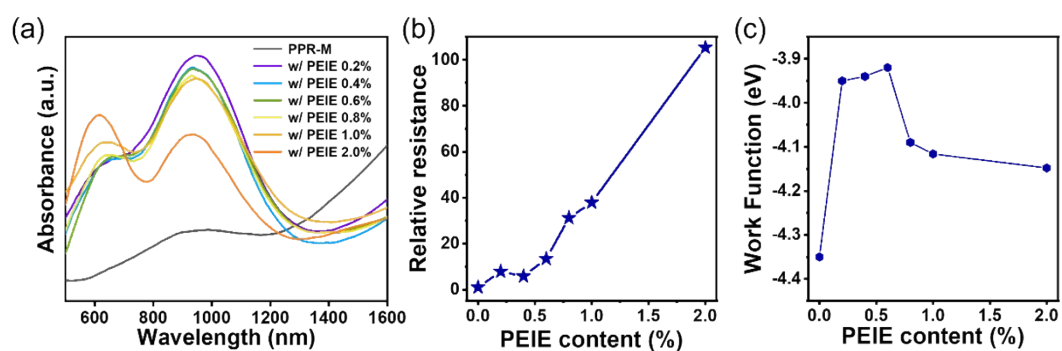


**Fig. S8** (a) UV-vis-NIR absorption spectra of PPR-M films decorated by spin-coating of PEIE solution with different concentrations. (b) Relative resistance and (c) work function of PEIE-modified PPR-M films.

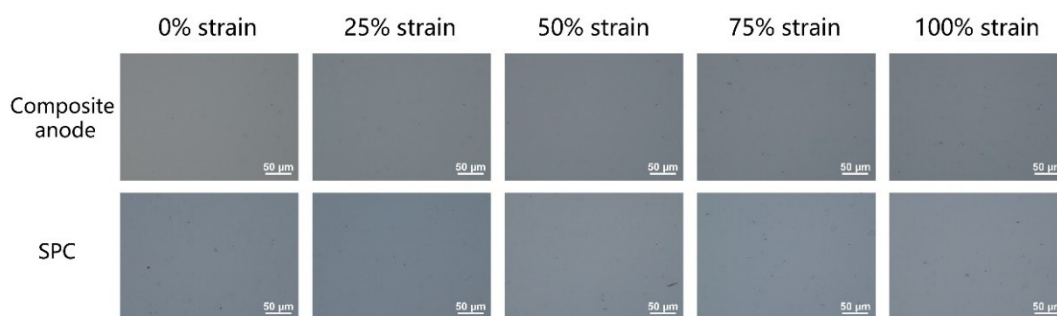


**Fig. S9** Optical microscope images of composite anode and SPC films under stretching.



## 5. Mechanical properties of DPS films

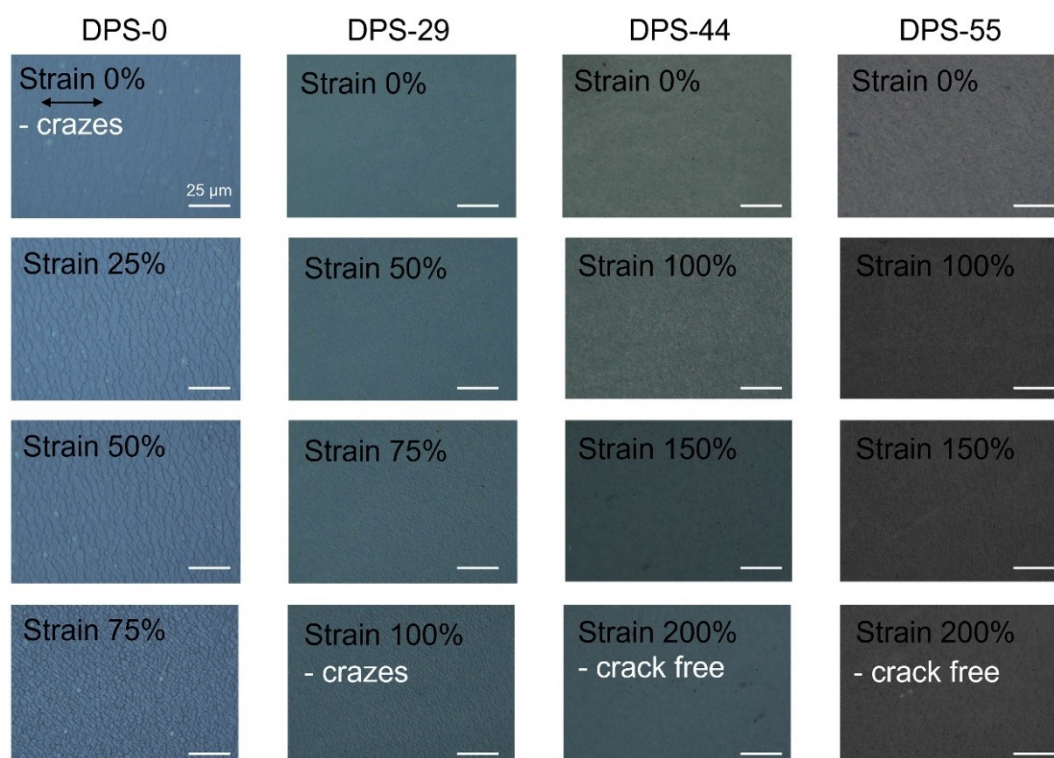


**Fig. S10** Optical microscope images of DPS-x films under different strains.



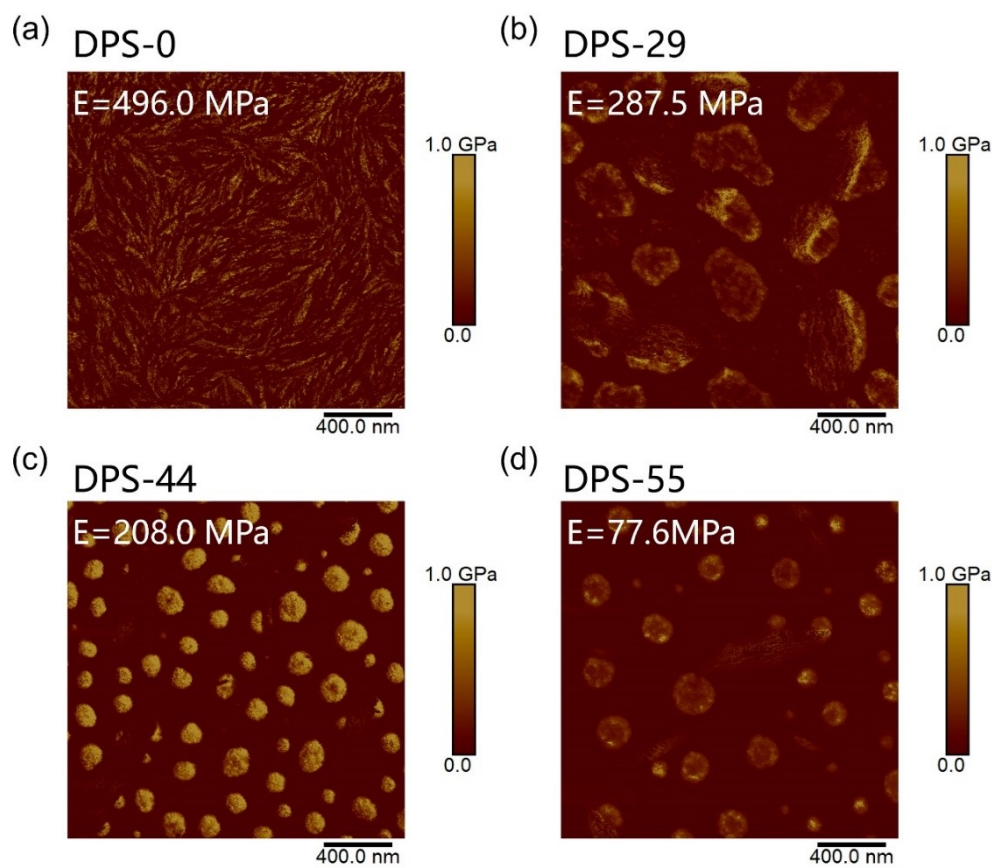


**Fig. S11** DMT modulus images of DPS-x films obtained by PFQNM.

## 6. Characterizations of OPD devices on rigid substrates

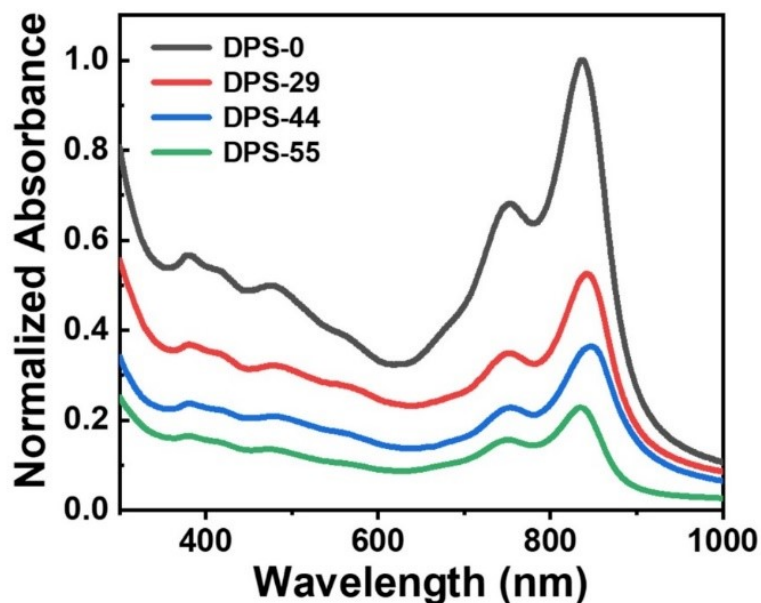


Fig. S12 UV-vis absorption spectra of DPS-x films.

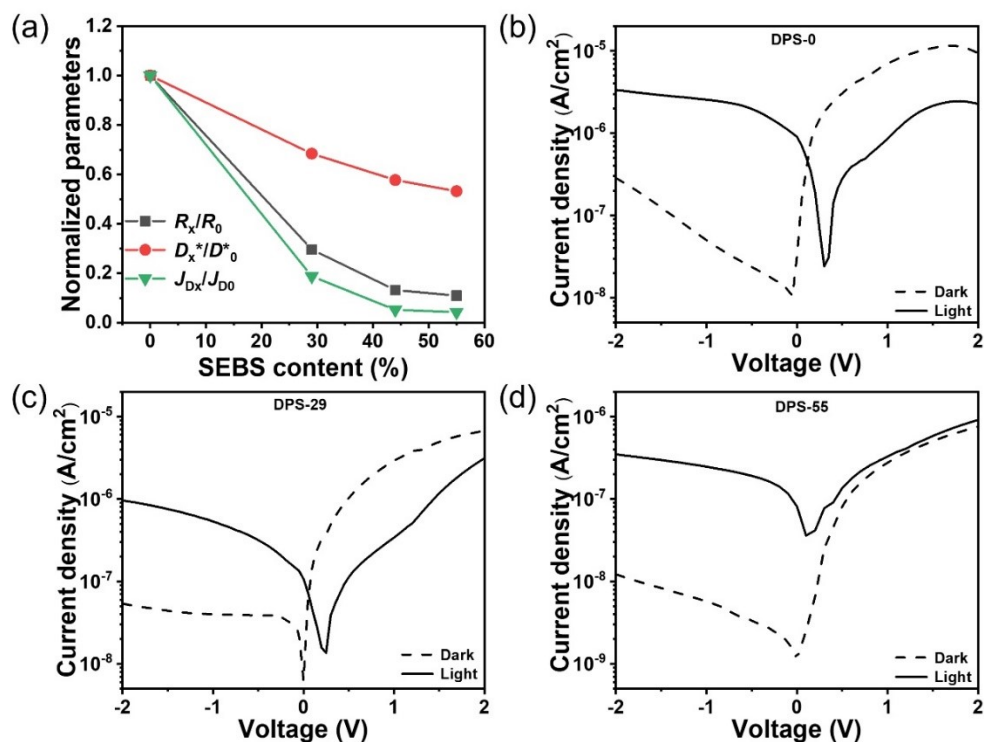
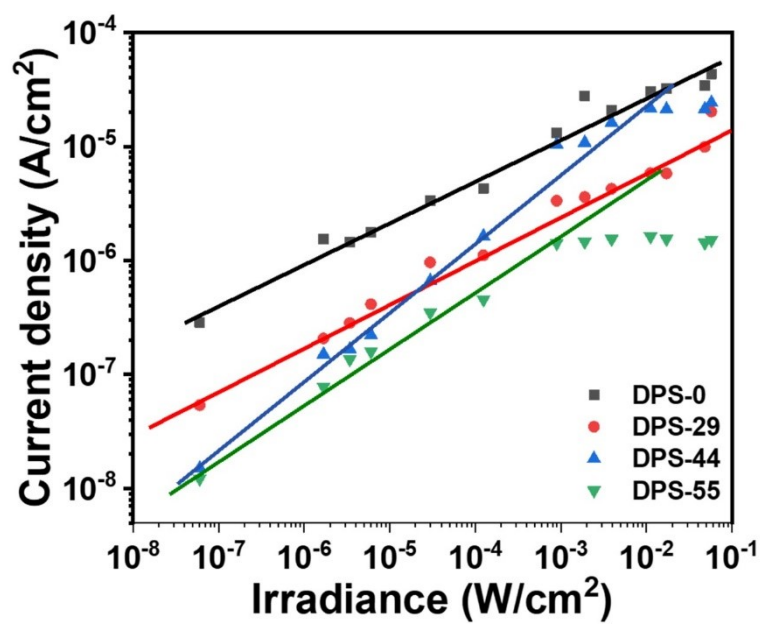
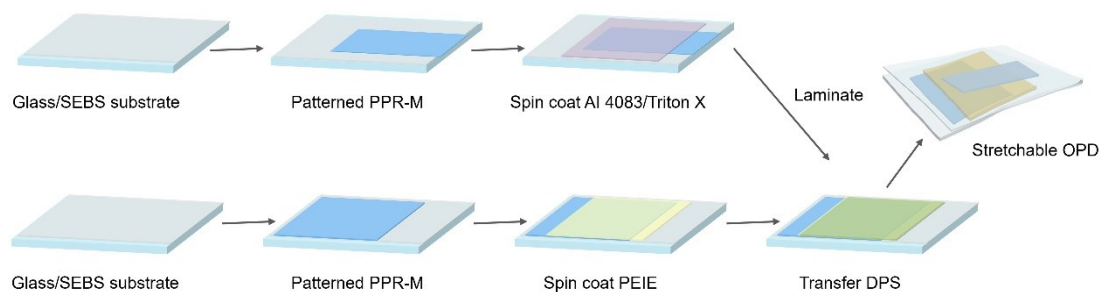


Fig. S13 (a) Normalized parameters of rigid OPDs as a function of SEBS content.  $x$  represents the percentage of SEBS content.  $J$ - $V$  characteristics of devices of (b) DPS-0, (c) DPS-29 and (d) DPS-55 under dark and irradiation at 808 nm ( $35.5 \mu\text{W}/\text{cm}^2$ ).



**Fig. S14** Linear dynamic range (LDR) for OPDs on rigid substrates measured at 808 nm.

## 7. Characterizations of stretchable OPD devices



**Fig. S15** Fabrication process of an intrinsically stretchable OPD.

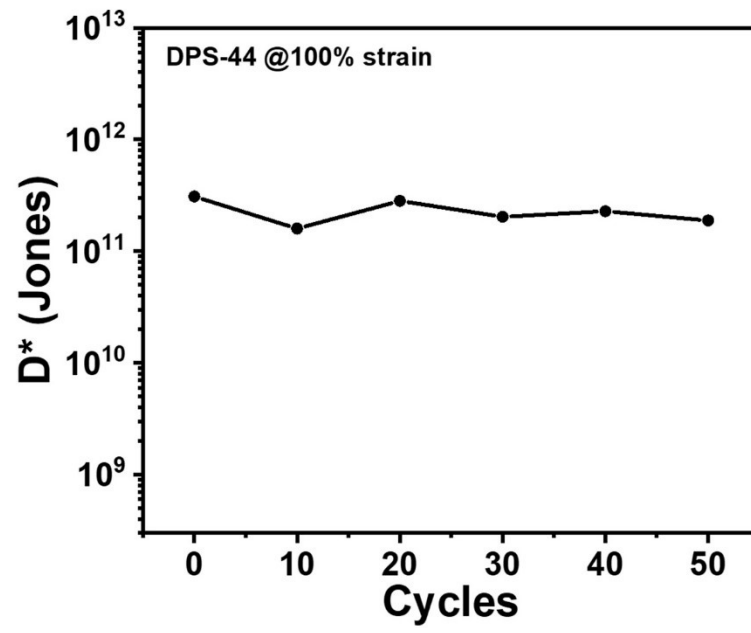


**Fig. S16** Cyclic stretching test on  $D^*$  between 0 and 100% strain.

## 8. References

- 1 Y. Jiang, Z. Zhang, Y.-X. Wang, D. Li, C.-T. Coen, E. Hwaun, G. Chen, H.-C. Wu, D. Zhong, S. Niu, W. Wang, A. Saberi, J.-C. Lai, Y. Wu, Y. Wang, A. A. Trotsyuk, K. Y. Loh, C.-C. Shih, W. Xu, K. Liang, K. Zhang, Y. Bai, G. Gurusankar, W. Hu, W. Jia, Z. Cheng, R. H. Dauskardt, G. C. Gurtner, J. B.-H. Tok, K. Deisseroth, I. Soltesz and Z. Bao, *Science*, 2022, **375**, 1411-1417.
- 2 Y. Bai, W. Li, Y. Tie, Y. Kou, Y.-X. Wang and W. Hu, *Adv. Mater.*, 2023, **35**, 2303245.
- 3 Z. Zhang, W. Wang, Y. Jiang, Y.-X. Wang, Y. Wu, J.-C. Lai, S. Niu, C. Xu, C.-C. Shih, C. Wang, H. Yan, L. Galuska, N. Prine, H.-C. Wu, D. Zhong, G. Chen, N. Matsuhisa, Y. Zheng, Z. Yu, Y. Wang, R. Dauskardt, X. Gu, J. B. H. Tok and Z. Bao, *Nature*, 2022, **603**, 624-630.
- 4 C. Wang, X. Ren, C. Xu, B. Fu, R. Wang, X. Zhang, R. Li, H. Li, H. Dong, Y. Zhen, S. Lei, L. Jiang and W. Hu, *Adv. Mater.*, 2018, **30**, 1706260.